A Floating Random-Walk Algorithm based on Iterative Perturbation Theory: Solution of the 2D, Vector-Potential Maxwell-Helmholtz Equation

K. Chatterjee

Electrical and Computer Engineering Department
California State University, Fresno
Fresno, CA 93740-8030
Email: *kchatterjee@csufresno.edu*, Tel: (559) 278-6038, Fax: (559) 278-6297

Y. L. Le Coz

Department of Electrical, Computer, and Systems Engineering
Rensselaer Polytechnic Institute
Troy, NY 12180-3590
Email: *lecozy@rpi.edu*, Tel: (518) 276-2937, Fax: (518) 276-8761

ABSTRACT

At present multi-GHz operating frequencies, the electrical properties of high-end, multilevel IC interconnects must be described with Maxwell's equations. We have developed an entirely new floating random-walk (RW) algorithm to solve the 2D time-harmonic Maxwell-Helmholtz equation. The algorithm requires no numerical mesh, thus consuming a minimum of computational memory—even in complicated problem domains, such as those encountered in IC interconnects. The major theoretical challenge of deriving an analytical Green's functions in arbitrary heterogeneous problem domains has been successfully resolved by means of an accurate approximation: iterative perturbation theory. Initial numerical verification of the algorithm has been achieved for the case of a "skin-effect" problem within a uniform circular conductor cross section, and also for a heterogeneous "split-conductor" problem, where one segment of a square domain is conducting material, while the other segment is insulating. As an example of electrical parameter extraction using this algorithm, we have extracted the frequency-dependent impedance of the uniform circular cross-section previously mentioned. Excellent agreement has been obtained between the analytical and RW solutions, supporting the theoretical formulation presented here.

Index Terms—Floating random-walk, Helmholtz equation, Maxwell equations, perturbation theory, skin effect, IC interconnect.

I. INTRODUCTION

Advances in digital IC technology have resulted in multi-GHz operation frequencies. At such frequencies, circuit designers must account for electromagnetic phenomena that are difficult to calculate. They include skin-effect loss, frequency-dependent inductance and capacitance, slow-wave substrate coupling, distributed transmission-line propagation and high-frequency radiation. Our principal objective here is to invent a new numerical algorithm capable of efficiently describing these increasingly significant electromagnetic phenomena. Our hope is to establish a new approach for the modeling and design of complex, multilevel IC-interconnects.

Traditional numerical methods for solving electromagnetic problems, unfortunately, require a discretization mesh. Mesh size and the resultant difficulty of solution become somewhat unmanageable in complicated 3D problem domains. The random walk (RW) algorithm [1] that we present here does not employ a mesh. In essence, the algorithm executes a Monte Carlo integration [2] of an infinite series of multi-dimensional integrals by means of RWs through the problem domain. These integrals contain "surface" and "volume" Green's function kernels. Note, importantly, the RW method is inherently parallel, requiring minimal inter-processor communication.

A large portion of the traditional RW literature treats the Helmholtz equation in homogeneous problem domains [3]. This is principally because of the ab-

sence of an exact analytical Green's function in arbitrary heterogeneous domains [4]. The RW algorithm we present in this work, on the other hand is applicable to heterogeneous problem domains—essential for IC-interconnect modeling.

The primary objective of this work is the detailed theoretical formulation of a novel floating RW algorithm based on iterative perturbation theory. In Section II, we develop a vector-potential formulation of the 2D Maxwell-Helmholtz equation, suitable for skin-effect analysis. A derivation of the relevant Green's functions for the 2D Maxwell-Helmholtz equation using iterative perturbation theory is given in Section III. In Section IV, we apply the Green's functions defined in Section III to define a specific floating RW algorithm. Section V presents the results of a numerical 2D skin-effect problem analysis within a circular conductor cross section, including the frequency-dependence impedance per unit length for the circular cross section at different frequencies. This section also contains the results for a heterogeneous "split-conductor" problem, where one segment of a square cross section is electrically conducting, while the other is insulating. For each one of these problems, comparison with an exact, analytical solution is provided. Lastly, Section VI summarizes our work and indicates possible future directions.

II. PROBLEM FORMULATION

Consider a 2D solid-conductor cross section in the *xy* plane, where we impress a *z*-directed current density at the conductor surface. We define a corresponding current-density phasor J_z in the harmonic steady state. We, furthermore, neglect any free-charge density as an approximation. Time-harmonic Maxwell's equations require that the electric-field phasor within the conductor cross section satisfy the scalar Helmholtz equation [5]:

$$\nabla^2 E_z - \gamma^2 E_z = 0. \tag{1}$$

Above, $\nabla^2 = \partial^2/\partial x^2 + \partial^2/\partial y^2$; $E_z = E_z(x, y)$; $\gamma^2 = -\mu_0 \varepsilon \omega^2 + i\mu_0 \sigma \omega$; ω, μ_0, ε and σ are operation frequency, free-space magnetic permeability, permittivity and conductivity, respectively. At the conductor surface, the impressed current density expresses itself as a boundary condition in electric field by means of the Ohm's Law constitutive relation:

$$E_z = \frac{J_z}{\sigma}. \tag{2}$$

Equations (1) and (2) essentially describe the so-called 2D "skin-effect problem" in our conductor. Electric field, or equivalently, current density, will vary within the conductor as a function of frequency and material parameters, subject to an applied surface boundary condition. We choose now to reformulate the problem, using vector potential $\mathbf{A} = A_z(x, y)\hat{\mathbf{e}}_z$, with $\nabla \times \mathbf{A} = \mathbf{B}$ in the Coulomb gauge $\nabla \cdot \mathbf{A} = 0$ [6]. This formulation is useful in a future 3D extension of this work, because it conveniently decouples field components in the governing equations.

Equations (1) and (2), in the vector-potential formulation, generate a "forced" Maxwell-Helmholtz system:

$$\nabla^2 A_z - \gamma^2 A_z = -\mu_0 \sigma \frac{\partial \varphi}{\partial z}, \tag{3}$$

$$J_z = -i\sigma\omega A_z - \sigma \frac{\partial \varphi}{\partial z}, \tag{4}$$

where, at the conductor surface,

$$A_z = 0. \tag{5}$$

The quantity $-i\sigma\omega A_z$ above is the so-called "eddy-current density". In deriving (3) and (4) from Maxwell's equations, we observe that for no free-charge density, the scalar potential function φ is frequency independent and it is completely decoupled from vector potential A_z.

In addition, as $\partial\varphi/\partial z$ generally depends solely on *x* and *y*, and not ω, it must, as well, satisfy (4) in the dc limit $\omega \to 0$. Accordingly, $-\sigma\partial\varphi/\partial z$ can be identified as the dc current density phasor. It should be noted, that though this phasor has a non-constant harmonic temporal variation $\exp(i\omega t)$ for any $\omega \neq 0$, its spatial dependence remains identical to that at dc.

We require, as well, correspondence with surface condition (2). We must be careful, therefore, to impress a surface current density in (2) consistent with (4) and (5). In other words, we define an ideal source as one that excites our conductor cross section according to (4) and (5). An ideal source maintains the

dc current-density phasor spatial dependence at the conductor surface, with the proviso that the phasor temporal dependence is of the form $\exp(i\omega t)$.

III. ITERATIVE PERTURBATION THORY BASED GREEN'S FUNCTION

The Green's function equation corresponding to the 2D Maxwell-Helmholtz equation (3) is

$$\nabla^2 G - \gamma^2 G = \delta(\mathbf{r} - \mathbf{r_o}), \tag{6}$$

where $G = G(\mathbf{r} \mid \mathbf{r_o})$ is the Green's function at (x, y) position coordinate $\mathbf{r}$ due to a 2D Dirac delta-function source at $\mathbf{r}_o$. Equation (6) does not, generally, have an analytical solution for arbitrary $\gamma(\mathbf{r})$. We will derive, nonetheless, using iterative perturbation theory [7], an approximate expression for G on the circular domain, with arbitrary radius R, shown in Fig. 1. This Green's function will allow us to later develop a novel RW algorithm for the solving 2D skin-effect equation (3). The Green's function G is assumed to be zero on the boundary of the circular domain, as the problems under consideration are Dirichlet [8] problems.

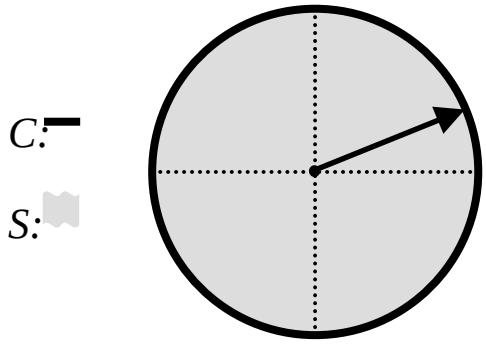

Figure 1: A circle of arbitrary radius R over which the Green's function in (6) is estimated.

Let us define the zeroth-order approximation $G^{(0)}$ for G as the solution to (6) with $\gamma = 0$. Therefore,

$$\nabla^2 G^{(0)} = \delta(\mathbf{r} - \mathbf{r_o}). \tag{7}$$

Above, $\mathbf{r}$ (ρ, θ) is the point where the zeroth-order approximation is calculated given a delta function centered at $\mathbf{r_o}$ (ρ_o, θ_o).

Using (6) for iteration, we can then generate a first-order approximation $G^{(1)}$ in terms of $G^{(0)}$:

$$\nabla^2 G^{(1)} = \delta(\mathbf{r} - \mathbf{r_o}) + \gamma^2 G^{(0)}. \tag{8}$$

The solution to Poisson equation (7) is well known; it has the form, in polar coordinates [9]

$$\begin{aligned} G^{(0)} &= \frac{1}{4\pi} \ln\left[R^2 \frac{A}{B} \right]. \\ A &= \rho^2 + \rho_o^2 - 2\rho\rho_o \cos(\theta - \theta_o). \\ B &= \rho^2 \rho_o^2 + R^4 - 2\rho\rho_o R^2 \cos(\theta - \theta_o). \end{aligned} \tag{9}$$

Now, we are in a position to evaluate $G^{(1)}$ from (8). Using the expression for $G^{(0)}$, and with the right side of (8) as the Poisson source term, we find an expression for the first-order approximation to (6) given by [10]

$$\begin{aligned} G^{(1)}(\mathbf{r} \mid \mathbf{r_o}) &= \iint_S d^2 r_S G^{(0)}(\mathbf{r} \mid \mathbf{r}_S) \\ &\left[\delta(\mathbf{r}_S - \mathbf{r_o}) + \gamma^2(\mathbf{r}_S) G^{(0)}(\mathbf{r}_S \mid \mathbf{r_o}) \right] \\ &= G^{(0)}(\mathbf{r} \mid \mathbf{r_o}) + \\ &\iint_S d^2 r_S \; \gamma^2(\mathbf{r}_S) G^{(0)}(\mathbf{r} \mid \mathbf{r}_S) G^{(0)}(\mathbf{r}_S \mid \mathbf{r_o}). \end{aligned} \tag{10}$$

Note that $G^{(1)}$ given by (10), is an approximate expression for G as given by (6). The integration variable in (10) represents an infinitesimal area element on the circular-domain surface S in Fig. 1. Note, as mentioned earlier, homogeneous Dirichlet conditions have been employed in obtaining (9) and (10).

We next use this approximate Green's function $G^{(1)}$ to develop a general solution to skin-effect equation (3) within our circular domain in Fig. 1. Two integral terms arise—a line integral about the domain circumference C which takes into account the effect of boundary conditions, and a surface integral throughout the domain S itself, which takes into account the effect of the source term, and the vector-potential at the center of the circular domain is given by [11]

$$A_z\,\textbf{(center)} = \oint_C A_z(R,\theta)\nabla_{\mathbf{r_o}} G(\mathbf{r}\,|\,\mathbf{r_o})\cdot\hat{\mathbf{n}}dc + \iint_S \left(-\mu_o\sigma\frac{\partial\phi}{\partial z}\right)G(\mathbf{r}\,|\,\mathbf{r_o})ds. \tag{11}$$

Substituting (10) in (11) and after some mathematical manipulation, we obtain, for A_z at the domain center

$$A_z\,\textbf{(center)} \approx \int_0^{2\pi} d\theta\, A_z(R,\theta)\left[\frac{1}{2\pi}+\frac{1}{4\pi^2}\sum_q W_q(\theta)\right] - \left(\mu_0\sigma\frac{\partial\varphi}{\partial z}\right)\int_0^R d\rho\int_0^{2\pi} d\theta\,\rho\left[\frac{1}{2\pi}\ln(\rho/R)+\frac{1}{8\pi^2}\sum_q F_q(\rho,\theta)\right] \tag{12}$$

where

$$W_q(\theta) = \gamma_q^2\int_0^R d\eta\int_{(q-1)\pi/2}^{q\pi/2} d\xi\,\frac{C}{D}$$
$$C = \eta\ln(\eta/R)(R^2-\eta^2) \tag{13}$$
$$D = R^2+\eta^2-2R\eta\cos(\theta-\xi).$$

and

$$F_q(\rho,\theta) = \gamma_q^2\int_0^R d\eta\int_{(q-1)\pi/2}^{q\pi/2} d\xi\,\eta\ln(\eta/R)\ln\left[\frac{E}{F}\right]$$
$$E = \rho^2R^2+\eta^2R^2-2\rho\eta R^2\cos(\theta-\xi) \tag{14}$$
$$F = \rho^2\eta^2+R^4-2\rho\eta R^2\cos(\theta-\xi).$$

For simplicity, above, we take γ^2 to be piecewise constant with respective values γ_q in θ-quadrants q = 1, 2, 3, and 4. The quantities within square brackets in (12) are 2D versions, respectively, of surface and volume Green's functions encountered in 3D problem domains. These Green's functions consist of two auxiliary functions W_q and F_q defined in (13) and (14). The functions represent perturbative corrections arising from the $\gamma^2 A_z$ term in the original Maxwell-Helmholtz equation (3). In (13) and (14), η and ξ are variables of integration. η takes values between 0 and R, while θ assumes values between $(q-1)\pi/2$ to $q\pi/2$ for a particular quadrant. Equations (12)–(14) are the starting point for defining a RW algorithm for solving (3) in 2D domains with arbitrary piecewise-constant spatial variation in γ, subject to arbitrary Dirichlet boundary conditions.

The total current, I, through the cross section can be calculated by integrating the current density given in (4) over the problem domain (ds being an infinitesimal area unit) and can be written as

$$I = \iint_S ds\left[-i\sigma\omega A_z - \sigma\frac{\partial\varphi}{\partial z}\right]. \tag{15}$$

The integral expression for vector potential from (12) is substituted in (15) to obtain a multi-dimensional integral expression for total current through the conductor surface.

The internal impedance per unit length is defined as[12]

$$Z_i = \frac{E_z(dc\ value) = \dfrac{\partial\varphi}{\partial z}}{I}. \tag{16}$$

At this point, the crucial thing to note is that for estimating frequency-dependent impedance, we need not estimate field or vector potential at a large number of points within the problem domain, or for that matter, at any point within the problem domain. The problem of impedance extraction is reduced to estimating the overall multi-dimensional integral expression for current obtained from (15) within the FRW framework to be described in the next section, and then using (16) to evaluate the internal impedance per unit length.

IV. THE FLOATING RW ALGORITHM

As mentioned earlier, the floating RW algorithm is a Monte Carlo evaluation of an infinite series of multi-dimensional integrals. The kernels of these integrals consist of products of surface and volume Green's functions. In this section, we describe the floating RW algorithm in detail in context of the skin-effect problem in a circular cross section. As shown in Fig.

2, we define RWs to start at a point, where we need to estimate A_z in (3).

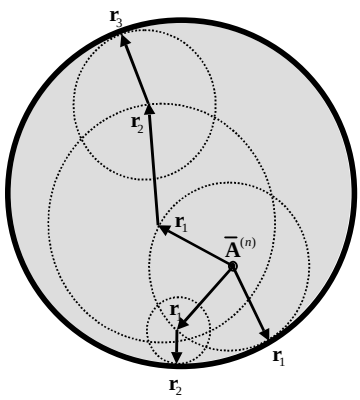

Figure 2: A schematic diagram of a circular cross section is shown. One-, two- and a three- hop RWs are represented.

The RWs propagate as "hops" of different sizes from circle centers to circumferences, consistent with a statistical interpretation [1] of (12). Maximally sized circles, subject to limitations imposed by iterative perturbation theory, are used with hop-location probability rules again consistent with (12).

We define, with each hop, a numerical weight factor derived from (12). The product of these weight factors over a walk, multiplied by the solution at the problem boundary—where the walk must terminate—gives a statistical estimate for A_Z at the RW starting point. All this, again, is entirely consistent with a statistical interpretation of (12). We can thus obtain an accurate statistical estimate for A_Z by averaging over a statistically large number of RWs. Mathematically, we can write such an estimate

$$\overline{A}_z \approx \frac{1}{N}\sum_{n=1}^{N}\overline{A}_Z^{(n)}, \tag{17}$$

where *N* is the number of walks and $\overline{A}_z^{(n)}$ is the *n*th-walk estimate. Referring, again, to Fig. (2), we see examples of three representative RWs: a one-hop, a two-hop, and a three-hop walk. The contributions from these three RWs can be written as

$$\begin{aligned}
\overline{A}_z^{(1)} &= K_S(\mathbf{r}_1),\\
\overline{A}_Z^{(2)} &= K_S(\mathbf{r}_1) + K_C(\mathbf{r}_1)K_S(\mathbf{r}_2),\\
\overline{A}_z^{(3)} &= K_S(\mathbf{r}_1) + K_C(\mathbf{r}_1)K_S(\mathbf{r}_2) +\\
&\quad K_C(\mathbf{r}_1)K_C(\mathbf{r}_2)K_S(\mathbf{r}_3).
\end{aligned} \tag{18}$$

Above, K_C represents the weight factor associated with the "surface" Green's function, the θ-integral term in (12). The function K_S represents the weight factor associated with the "volume" Green's function, the (ρ,θ)-integral term in (11). Assuming the hops are uniformly distributed in (ρ,θ), these weight factors have the form, from (12),

$$K_C = R\left(1+\frac{1}{2\pi}\sum_q W_q(\theta)\right) \tag{19}$$

and

$$\begin{aligned}
K_S = &-\left(\mu_0\sigma\frac{\partial\varphi}{\partial z}R^2\right)\\
&\left[\frac{1}{2}\ln(\rho/R)+\frac{1}{8\pi}\sum_q F_q(\rho,\theta)\right].
\end{aligned} \tag{20}$$

For estimating the frequency-dependent impedance per unit length as given in (16) a similar exercise is carried out using a statistical interpretation of (15). For heterogeneous problems, there are a couple of differences. First of all, the maximum hop size, which is decided by the validity of iterative perturbation theory, is different for different medium. In this paper, the maximum hop size is estimated to be the minimum of two numbers. First, we allow the first-order correction in the expression for the volumetric Green's function given in (12) to be equal to ten percent of the zeroth-order approximation and calculate a maximum hop size under this assumption. A similar process is carried out for the surface Green's function term in (12) and a maximum hop size is calculated under this assumption. The maximum hop size for our RW algorithm is the smaller of these two numbers. Secondly, the random hops are restricted by material interfaces in heterogeneous problems.

We close this section with a pseudo-code listing that defines our floating RW algorithm for estimating vector-potential.

—Floating Random-Walk Algorithm Pseudo-Code—

1) *Choose the point where A_z need be estimated; call it* AZ.
2) *Evaluate* δ' = the maximum hop size as determined by validity of perturbation theory, according to the procedure described previously in this section.
3) Δ = *a pre-defined small number*.
4) NMAX = *a pre-defined large integer*.
5) N = 0.
6) TOTAL_SUM = 0.
7) SUM = 0.
8) *Evaluate the maximal radius that contacts the closest problem-domain boundary, without passing through it; call it* RMAX.
9) RAD = MIN (RMAX, δ').
10) *Draw a circle of radius* RAD.
11) *Hop to a point on the circumference in conformity with a uniform probability distribution in* θ.
12) *Evaluate the exact weight factor K_C from (13)* and *(19);* call it KC.
13) *Evaluate the exact weight factor K_S from (14)* and *(20);* call it KS.
14) KC (*zeroth hop*) = 1; INCREMENT = KC (*previous hop*) * KS (*present hop*).
15) SUM = SUM + INCREMENT.
16) IF (*a boundary is not reached*) THEN (*repeat steps 8 –15*).
17) IF (*a boundary is reached*) THEN (*terminate walk*; N = N + 1; SUM_TOTAL = SUM_TOTAL + SUM).
18) IF (N < NMAX) THEN (*repeat Steps 7–17*).
19) IF (N $\geq$ NMAX) THEN (AZ = SUM_TOTAL / NMAX).
20) *Evaluate exact, analytical solution* AZ(exact).
21) ERROR = $\left|\text{AZ} - \text{AZ(exact)}\right|$.
22) IF (ERROR > Δ) THEN (NMAX = NMAX * 1.2; *repeat steps 5 –21*).
23) IF (ERROR $\leq \Delta$) THEN (AZ = *estimated value of A_z*).

V. VERIFICATION WITH THE HELP OF BENCHMARK PROBLEMS

The principal objective of this work is to formulate and to define a novel RW algorithm for 2D Maxwell-Helmholtz equation solution. We have benchmarked our formulation against two known solutions. As said earlier, the first problem is a single circular cross section, where an alternating current of single frequency is impressed. Using the algorithm developed earlier, we estimate the current density profile across the cross section as well as the internal impedance. The analytical solution for the current density along a uniform, circular-conductor cross section of radius *R* is [12]

$$\frac{J_z(\rho)}{J_z(0)} = \frac{J_0(i\gamma\rho)}{J_0(i\gamma R)}, \tag{21}$$

where J_0 is the zeroth-order Bessel function. The variable ρ here denotes radial coordinate from the conductor center. For this circular cross section, an analytical expression for the internal impedance per unit length as defined in (16) is given by [12]

$$Z_i = -\frac{i\gamma J_0(i\gamma R)}{2\pi R\sigma J_0'(i\gamma R)}. \tag{22}$$

As mentioned earlier, the second problem solved is a heterogeneous "split-conductor" problem, where a square domain is divided into two unequal rectangular domains of insulating and conducting material, as shown in Fig. (3).

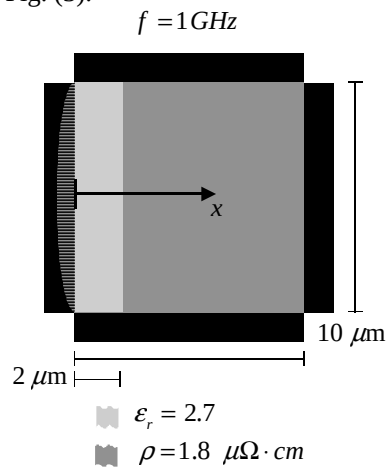

Figure 3: 2D, split-conductor problem, the geometry.

The insulating region is represented in light gray, while the conducting region is represented in dark gray. The boundary regions, where the *z*-component of the vector potential is known, are represented in black. The boundary conditions are chosen such that $A_z = 0$ in the top, bottom and right boundary regions, while $A_z = \sin(\pi y / L)$ in the left boundary region (L being the length of the side of the square) where the origin coincides with the left and bottom corner. Assuming the continuity of the solution and its derivative at the material interface (L_0 being the length of the dielectric), the analytical solution to this heterogeneous problem is given by [13]

$$\begin{array}{c} A_z = \sin(ky) \\ \left[A\sinh(k_d x) + \cosh(k_d x)\right], 0 \le x < L_0. \\ A_z = \sin(ky) \\ \left[C\sinh\{k_c (x-L)\}\right], L_0 \le x < L. \end{array} \tag{23}$$

The constants in (23) are given in (24) and (25) as:

$$\begin{aligned} k &= \frac{\pi}{L}. \\ k_d &= \sqrt{\gamma_d^2 + k^2}. \\ k_c &= \sqrt{\gamma_c^2 + k^2}. \\ A &= \frac{\begin{vmatrix} a_3 & a_2 \\ b_3 & b_2 \end{vmatrix}}{\begin{vmatrix} a_1 & a_2 \\ b_1 & b_2 \end{vmatrix}}. \\ C &= \frac{\begin{vmatrix} a_1 & a_3 \\ b_1 & b_3 \end{vmatrix}}{\begin{vmatrix} a_1 & a_2 \\ b_1 & b_2 \end{vmatrix}}. \end{aligned} \tag{24}$$

$$\begin{array}{c} a_1 = \sinh(k_d L_0), a_2 = -\sinh\left[k_c (L_0 - L)\right], \\ a_3 = -\cosh(k_d L). \\ b_1 = \sqrt{\varepsilon} a_1, b_2 = \sqrt{\frac{-j\sigma}{\omega}} a_2, b_3 = \sqrt{\varepsilon} a_3. \\ \gamma_d^2 = -\mu\varepsilon\omega^2, \gamma_c^2 = i\mu\sigma\omega. \end{array} \tag{25}$$

We coded the algorithm in MATLAB 5.0™, using a 400-MHz Apple PowerBook G3™ development platform. The resistivity for conducting material is given by $\rho = 1.8\,\mu\Omega - \text{cm}$ and relative permittivity of dielectric material is given by $\varepsilon_r = 2.7$. The radius of the circular cross section is given by $R = 5\mu$m while for the split-conductor problem, the dimensions of the square cross section is given by $10\,\mu\text{m} \times 10\,\mu\text{m}$. The respective dimensions of the insulating and the conducting materials in the split-conductor problems are shown in Fig. (3). The operating frequency $f = \omega/2\pi = 1$GHz corresponds to a skin depth $\delta_s = 2.1\mu$m and a wavelength of $1.8\times10^5\,\mu$m. The propagation-constant squared (γ^2) is equal to $4.386\times10^{11} i/\text{m}^2$ within the conductor and equal to $-1185.431197\text{m}^{-2}$ within the dielectric at 1 GHz. Based on these numbers and the criterion given in Section IV, the maximum radius of hops inside conducting material is 0.95μm, and the maximum radii of hops within the dielectric material is $1.8\times10^4\,\mu$m, which is about twice the dimensions of a chip (based on a 1 cm×1cm chip). Thus we see that this perturbation theory based approach has the potential to allow meaningful interconnect analysis.

Figures (4) and (5) show the magnitude ratio and phase lag, respectively, of the skin-effect current density phasor. A total of 20,000 RWs were performed per solution point. The figures show excellent agreement between the analytical and RW solutions. The mean absolute error between exact and RW solutions was 0.001 for magnitude and 0.012rad for phase.

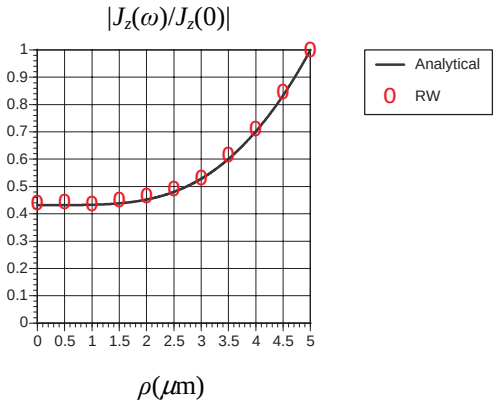

Figure 4: 2D skin-effect problem in a homogeneous circular conductor cross section, relative magnitude. Problem radius $R = 5\mu$m and $\omega = 1$GHz.

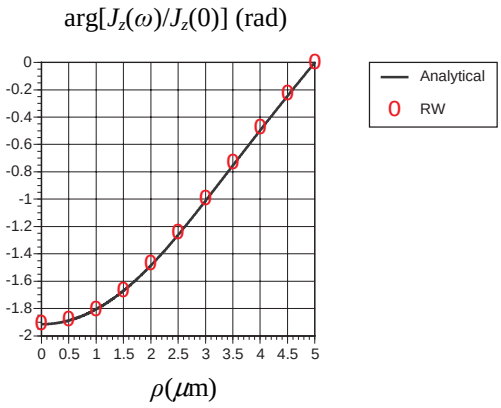

Figure 5: 2D skin-effect problem in a homogeneous circular conductor cross section, phase lag. Problem radius R = 5μm and ω = 1GHz.

As expected, the total current density is maximum and equal to the dc value at the boundary, and reaches its minimum at the center of the cross section. The characteristic skin-depth decay scale is well in evidence in Fig. (4). In addition, the expected maximum phase lag occurs at $\rho = 0$ in Fig. (5). Table (1) summarizes the results for the skin-effect problem, while Table (2) shows the results for the frequency-dependent self impedance of a cross section of radius 1.0 μm at frequencies of 1 GHz, 5 GHz and 10 GHz. As expected, both the frequency-dependent inductance and frequency dependent inductance increases with frequency. For extracting impedance, a total of only 1,000 RWs were performed per points. It can be seen from Table (2), that the error in the estimate of frequency-dependent resistance and inductive impedance is around 1 percent in all three cases. Table (3) summarizes the results for the heterogeneous problem, while Figures (6) and (7) illustrates the results for the same. Again, excellent conformity was obtained between the analytical and RW solutions.

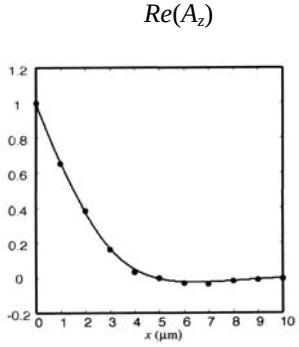

Figure 6: 2D, split-conductor problem, the real part of the solution.

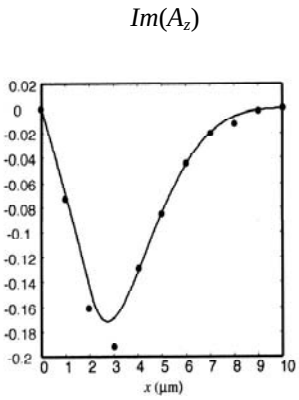

Figure 7: 2D, split-conductor problem, the imaginary part of the solution.

Frequency (GHz)	Random Walks Per Solution Point	Mean Absolute Error For Relative Magnitude	Mean Absolute Error For Relative Phase
1	20000	0.001 on a solution range (0·42 – 1·0).	0.012 on a solution range (–1·9 – 0).

Table 1: Numerical results for the 2D skin-effect problem in a circular conducting cross section.

Frequency (GHz)	Time (Seconds)	Analytical Result (Ω/m)	RW Result (Ω/m)	Error (Ω/m)
1	20	5735 + 314i	5738 + 312i	3 - 2i
5	30	5870 + 1552i	5917 + 1534i	47 - 18i
10	45	6262 + 2997i	6315 + 2962i	53 - 35i

Table 2: Numerical results for the frequency-dependent self-impedance of a conducting circular cross section.

Frequency (GHz)	Random Walks Per Solution Point	Mean Absolute Error for the Real Part of the Solution	Mean Absolute Error for the Imaginary Part of the Solution
1	2500	0.005 Solution range: –0·02 – 1·0.	0.005 Solution Range: –0·17 – 0·0.

Table 3: Numerical results for the "split-conductor" heterogeneous benchmark problem.

We will finish our discussion in this section by making a few comments on the accuracy of the solution, time and memory requirement. We have already observed the close agreement of the RW results with that of known analytical solutions. The accuracy of the solution of the solution can be enhanced by simply increasing the number of RWs as the error is proportional to $1/\sqrt{N}$, N being the number of RWs. This particular fact is a direct consequence of Central Limit Theorem [14]. The memory requirements for this technique are low as this approach does not require any numerical meshing. The time requirements of this algorithm can be further reduced by the use of variance-reduction techniques [2] and by parallelization. We plan to investigate all these issues in detail after we have applied our algorithm to more complicated structures.

VI. CONCLUSION

We have presented the theoretical basis of a novel floating RW algorithm for solving the 2D Maxwell-Helmholtz equation. The algorithm employs iterative perturbation theory. We have, as well, verified the algorithm's integrity by applying it to a homogeneous and a heterogeneous problem, possessing analytical solutions. The applicability to heterogeneous problems is a significant improvement on existing RW algorithms, an application we wish to explore further in our future work. Our algorithm can be readily extended to multi-conductor systems in full 3D. In this work, we have further demonstrated that this algorithm can be used to extract electrical parameters such as frequency-dependent impedance. We believe that with additional development, the algorithm may prove useful for electromagnetic analysis of complex, multilevel IC-interconnect structures.

Importantly, the algorithm is fully parallel. Thus, we expect significant performance acceleration in any future parallel software or hardware implementation.

Acknowledgement - This work has been sponsored by the Defense Advanced Research Projects Agency (DARPA); the New York State Office of Science, Technology, and Academic Research (NYSTAR); and the Semiconductor Research Corporation (SRC) Microelectronics Advanced Research Corporation (MARCO). The authors sincerely thank the sponsors for their support of this work.

REFERENCES

[1] Y.L. Le Coz and R.B. Iverson, "A Stochastic Algorithm for High Speed Capacitance Extraction in Integrated Circuits", *Solid-State Electronics*, vol. 35, pp. 1005–12, 1992.

[2] Ilya M. Sobol, *A Primer for the Monte Carlo Method*, Boca Raton, FL: CRC Press, 1994.

[3] K.K. Sabelfeld, *Monte Carlo Methods in Boundary Value Problems*, New York, NY: Springer-Verlag, 1991.

[4] K. Chatterjee, *Development of a Floating Random-Walk Algorithm for Solving Maxwell's Equations in Complex IC-Interconnect Structures*, pp. 28–31, Doctoral Thesis, Rensselaer Polytechnic Institute, Troy, NY, April 2002.

[5] D.M. Pozar, *Microwave Engineering, 2nd Edition*, pp. 16-7, New York, NY: John Wiley & Sons, 1998.

[6] J.D. Jackson, *Classical Electrodynamics, 3rd Edition*, pp. 241-2, New York, NY: John Wiley & Sons, 1999.

[7] Van Dyke, *Perturbation Methods in Fluid Mechanics*. Stanford, CA: Parabolic Press, 1975.

[8] R. Haberman, *Elementary Applied Partial Differential Equations with Fourier Series and*

Boundary Value Problems, 3rd Edition, pp. 155-7, Upper Saddle River, NJ: Prentice Hall, 1998.

[9] R. Haberman, *Elementary Applied Partial Differential Equations with Fourier Series and Boundary Value Problems, 3rd Edition*, pp. pp. 420-1, Upper Saddle River, NJ: Prentice Hall, 1998.

[10] R. Haberman, *Elementary Applied Partial Differential Equations with Fourier Series and Boundary Value Problems, 3rd Edition*, pp. 406-8, Upper Saddle River, NJ: Prentice Hall, 1998.

[11] R. Haberman, *Elementary Applied Partial Differential Equations with Fourier Series and Boundary Value Problems, 3rd Edition*, pp. 422-3, Upper Saddle River, NJ: Prentice Hall, 1998.

[12] S. Ramo, J. R. Whinnery, and T.V. Duzer, *Fields and Waves in Communication Electronics, 3rd Edition*, pp. 180-4, New York, NY: John Wiley & Sons, 1993.

[13 K. Chatterjee, *Development of a Floating Random-Walk Algorithm for Solving Maxwell's Equations in Complex IC-Interconnect Structures*, pp. 153-4, Doctoral Thesis, Rensselaer Polytechnic Institute, Troy, NY, April 2002.

[14] A. Papoulis and S.U. Pillai, *Probability, Random Variable and Stochastic Processes, 4th Edition*, McGraw Hill, 2001.

Kausik Chatterjee was born on 8 October, 1969. In June 1992, he received a Bachelor of Engineering degree in Electrical Engineering from Jadavpur University, Calcutta, India. Subsequently, in June, 1995, he received a Master of Technology degree in Nuclear Engineering from Indian Institute of Technology, Kanpur, India, and in May, 2002, he received his Ph.D degree in Electrical Engineering from Rensselaer Polytechnic Institute, Troy, New York. In August 2002, he joined the faculty, full-time, at California State University, Fresno as an Assistant Professor of Electrical and Computer Engineering. His current research interests include the development of stochastic algorithms for important equations in nature and a theory for high temperature superconductors. He has been awarded a Government of India Fellowship at Indian Institute of Technology, Kanpur, a University Fellowship at Ohio State University and an Intel Doctoral Fellowship. He has also received the Charles M. Close Doctoral Prize at Rensselaer Polytechnic Institute. He is a member of American Physical Society.

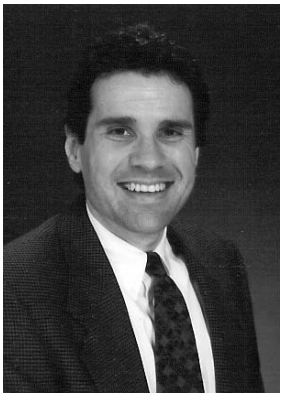

Yannick Louis Le Coz was born on 26 September 1958. In May 1980, he received a BS degree in Electrical Engineering from Rensselaer Polytechnic Institute, Troy, New York. Subsequently, in May 1982 and January 1988, respectively, he received M.S. and Ph.D. degrees in Electrical Engineering from the Massachusetts Institute of Technology, Cambridge, Massachusetts. His doctoral thesis, entitled "Semiconductor Device Simulation: A Spectral Method for Solution of the Boltzmann Transport Equation", was supervised by Prof. Alan L. McWhorter. In January 1988, he joined the faculty, full time, at Rensselaer Polytechnic Institute, as an Assistant Professor of Electrical, Computer, and Systems Engineering. He was awarded a tenured Associate Professorship in 1995. His research interests include transport in semiconductor devices, equilibrium heterojunction theory, and random-walk algorithms for the physical design of ICs. He is currently developing a novel random-walk algorithm for solving Maxwell's equations in complex, IC interconnect structures. With Dr. R.B. Iverson, he has also commercialized a random-walk IC-interconnect capacitance extractor *QuickCap*®, currently considered a "gold standard" in the chip-design industry. Dr. Le Coz has been a Digital Equipment Corporation Fellow, a Visiting Faculty at Sandia National Laboratories (Livermore, CA), a Connecticut State Scholar, and a General Motors Scholar. He has received the American Cyanamid, Perkin-Elmer, and Rensselaer Physics Awards. He is a member of Tau Beta Pi, Eta Kappa Nu, Sigma Xi, and the American Physical Society.